

# Variable temperature neutron diffraction study of crystal structure and transport pathways in oxide ion conductors $\text{Bi}_{12.5}\text{Ln}_{1.5}\text{ReO}_{24.5}$ (Ln=Lu, Er)

Hervoches, Charles H.; Greaves, Colin

DOI:

[10.1016/j.ssi.2013.10.032](https://doi.org/10.1016/j.ssi.2013.10.032)

License:

Creative Commons: Attribution (CC BY)

Document Version

Publisher's PDF, also known as Version of record

Citation for published version (Harvard):

Hervoches, CH & Greaves, C 2014, 'Variable temperature neutron diffraction study of crystal structure and transport pathways in oxide ion conductors  $\text{Bi}_{12.5}\text{Ln}_{1.5}\text{ReO}_{24.5}$  (Ln=Lu, Er)', *Solid State Ionics*, vol. 254, pp. 1-5. <https://doi.org/10.1016/j.ssi.2013.10.032>

[Link to publication on Research at Birmingham portal](#)

## Publisher Rights Statement:

Eligibility for repository : checked 04/06/2014

## General rights

Unless a licence is specified above, all rights (including copyright and moral rights) in this document are retained by the authors and/or the copyright holders. The express permission of the copyright holder must be obtained for any use of this material other than for purposes permitted by law.

- Users may freely distribute the URL that is used to identify this publication.
- Users may download and/or print one copy of the publication from the University of Birmingham research portal for the purpose of private study or non-commercial research.
- User may use extracts from the document in line with the concept of 'fair dealing' under the Copyright, Designs and Patents Act 1988 (?)
- Users may not further distribute the material nor use it for the purposes of commercial gain.

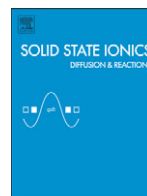
Where a licence is displayed above, please note the terms and conditions of the licence govern your use of this document.

When citing, please reference the published version.

## Take down policy

While the University of Birmingham exercises care and attention in making items available there are rare occasions when an item has been uploaded in error or has been deemed to be commercially or otherwise sensitive.

If you believe that this is the case for this document, please contact [UBIRA@lists.bham.ac.uk](mailto:UBIRA@lists.bham.ac.uk) providing details and we will remove access to the work immediately and investigate.



# Variable temperature neutron diffraction study of crystal structure and transport pathways in oxide ion conductors

## $\text{Bi}_{12.5}\text{Ln}_{1.5}\text{ReO}_{24.5}$ ( $\text{Ln} = \text{Lu}, \text{Er}$ )

Charles H. Hervoches<sup>\*</sup>, Colin Greaves

School of Chemistry, The University of Birmingham, Edgbaston, Birmingham, B15 2TT, United Kingdom

### ARTICLE INFO

#### Article history:

Received 25 March 2013

Received in revised form 12 September 2013

Accepted 17 October 2013

Available online 7 November 2013

#### Keywords:

Bismuth oxide

Fluorite structure

Oxide ion conductor

Neutron diffraction

Maximum entropy method

Diffusion path

### ABSTRACT

Samples of highly conducting  $\text{Bi}_{12.5}\text{Lu}_{1.5}\text{ReO}_{24.5}$  and  $\text{Bi}_{12.5}\text{Er}_{1.5}\text{ReO}_{24.5}$  have been studied by neutron powder diffraction at room temperature for both phases and at  $25^\circ\text{C} \leq T \leq 500^\circ\text{C}$  in the case of  $\text{Bi}_{12.5}\text{Er}_{1.5}\text{ReO}_{24.5}$ . Both materials crystallize in the cubic  $\delta\text{-Bi}_2\text{O}_3$  related system, space group Fm-3m. Changes in the oxygen sublattice at  $25^\circ\text{C} \leq T \leq 500^\circ\text{C}$  have been investigated by the Rietveld and maximum entropy methods.

© 2013 Elsevier B.V. All rights reserved.

## 1. Introduction

The high ionic conductor  $\delta\text{-Bi}_2\text{O}_3$  crystallises in a defect fluorite related structure, space group Fm-3m [1]. Its crystal structure is typically described with cations occupying the  $4a$  (0 0 0) position and oxygens in  $8c$  ( $\frac{1}{4}$   $\frac{1}{4}$   $\frac{1}{4}$ ) with some interstitial oxygens shifted towards ( $\frac{1}{2}$ ,  $\frac{1}{2}$ ,  $\frac{1}{2}$ ) [2], however slightly different systems to model the disordered distribution of the oxide ions have been proposed [3,4]. Its high ionic conduction is linked to the presence of ~25% oxygen ion vacancies in the structure [1,5]. The phase is stable only above  $730^\circ\text{C}$ , and attempts to stabilise the high oxide ion conductor  $\delta$ -phase at lower temperature have been the subject of numerous studies [6,7]. Amongst them, the stabilised  $\delta$ -phase family of compounds with composition  $\text{Bi}_{12.5}\text{Ln}_{1.5}\text{ReO}_{24.5}$  presents very high ionic conductivity at low temperature [8] and their detailed crystal structure characteristics appear to differ from those of  $\text{Bi}_2\text{O}_3$  doped with rare-earth only. In these materials, rhenium is apparently tetrahedrally coordinated at the local scale [9], while in the related ordered phase both tetrahedral  $\text{ReO}_4^-$  and octahedral  $\text{ReO}_6^{5-}$  species are present [10,11]. To date NPD data have been obtained only for  $T \leq 25^\circ\text{C}$ , and indicate significant differences in the O positions compared with conventional lanthanide stabilised phases: the interstitial oxygen position is significantly displaced and is thought

to be related to the enhanced conductivity [8]. In the present study we investigate the crystal structure of the  $\text{Bi}_{12.5}\text{Ln}_{1.5}\text{ReO}_{24.5}$  ( $\text{Ln} = \text{Lu}, \text{Er}$ ) system and the change in oxygen sublattice for  $25^\circ\text{C} \leq T \leq 500^\circ\text{C}$  in  $\text{Bi}_{12.5}\text{Er}_{1.5}\text{ReO}_{24.5}$ .

## 2. Experimental

Polycrystalline samples of  $\text{Bi}_{12.5}\text{Lu}_{1.5}\text{ReO}_{24.5}$  and  $\text{Bi}_{12.5}\text{Er}_{1.5}\text{ReO}_{24.5}$  have been prepared by traditional solid state synthesis from stoichiometric quantities of  $\text{Bi}_2\text{O}_3$ ,  $\text{Lu}_2\text{O}_3/\text{Er}_2\text{O}_3$ , and  $\text{NH}_4\text{ReO}_4$ . The powders were thoroughly mixed and ground, and subsequently heated in air at  $800^\circ\text{C}$  for 24 h with one intermediate grinding and allowed to cool slowly in the furnace.

X-ray powder diffraction (XRD) data were obtained at room temperature on a Siemens D5000 diffractometer operating in transmission mode (Ge primary beam monochromator giving  $\text{Cu-K}\alpha 1$  radiation, wavelength  $1.5406 \text{ \AA}$ ). Neutron powder diffraction (NPD) data of the samples were collected on the D2B diffractometer (wavelength  $1.5943 \text{ \AA}$ ) at the Institut Laue Langevin, Grenoble, France. Approximately 8 g of each material was loaded in a cylindrical vanadium can of 8 mm diameter for data collection at temperatures of  $25^\circ\text{C}$ ,  $200^\circ\text{C}$ ,  $300^\circ\text{C}$ ,  $400^\circ\text{C}$ , and  $500^\circ\text{C}$ .

Rietveld refinements were carried out using GSAS [12] with EXPGUI graphical user interface [13]. The nuclear density distribution was obtained by the maximum entropy method (MEM)/MEM-based pattern fitting (MPF) method using the program PRIMA [14] with  $128 \times 128 \times 128$  pixels in conjunction with Rietan-FP software [15].

<sup>\*</sup> Corresponding author at: Department of Neutron Physics, Nuclear Physics Institute v.v.i., ASCR, CZ-25068 Řež, Czech Republic. Tel.: +420 266172034.

E-mail address: [hervoches@ujf.cas.cz](mailto:hervoches@ujf.cas.cz) (C.H. Hervoches).

Crystal structures and nuclear density distribution representations were drawn with VESTA [16].

For electrical measurements, dense sintered pellet of approximately 8 mm diameter and 2 mm thickness were prepared and silver electrodes painted on both surfaces. Conductivity was measured over the temperature range 200–600 °C by a.c. impedance spectroscopy with a Solartron SI 1260 impedance analyzer in the frequency range 1 Hz to 10<sup>6</sup> Hz.

### 3. Results and discussion

XRD data confirmed the phase purity of the samples. As with other lanthanide doped bismuth rhenium oxides, they both adopt the cubic *Fm-3m* space group, lattice parameter  $a = 5.5592(1)$  Å and  $5.5697(1)$  Å for Bi<sub>12.5</sub>Lu<sub>1.5</sub>ReO<sub>24.5</sub> and Bi<sub>12.5</sub>Er<sub>1.5</sub>ReO<sub>24.5</sub> respectively at 25 °C.

Conductivity measurement (Fig. 1) demonstrated the high conductivity of the materials with values close to the ones previously reported [8]. Both materials have conductivity higher than Bi<sub>12.5</sub>Y<sub>1.5</sub>ReO<sub>24.5</sub> but lower than Bi<sub>12.5</sub>Nd<sub>1.5</sub>ReO<sub>24.5</sub> and Bi<sub>12.5</sub>La<sub>1.5</sub>ReO<sub>24.5</sub>. This follows the general trend of stabilized lanthanide doped δ-Bi<sub>2</sub>O<sub>3</sub>, which generally present higher conductivity with increased dopant ionic radius.

NPD data Rietveld refinements were performed using data from reference [8] based on δ-Bi<sub>2</sub>O<sub>3</sub> crystal structure as a starting model. Lattice parameter variation with temperature deviates from linearity (Fig. 2), which might indicate of a redistribution of oxide ions.

In their study of pure and Y-doped δ-Bi<sub>2</sub>O<sub>3</sub>, Battle et al. [2] observed the presence of interstitial oxygens on 32f (*xxx*) site in both cases, with another interstitial oxygen in 48i ( $\frac{1}{2}x\ x$ ) and displacement of cations to the 24e (*x* 0 0) site in the case of the Y-doped sample. Three oxygen positions (8c, 32f, 48i) were also reported with several lanthanide-doped Bi<sub>2</sub>O<sub>3</sub> by Boyapati et al. [17] and Y-doped Bi<sub>2</sub>O<sub>3</sub> by Abrahams et al. [18]; while in the Bi<sub>3</sub>Ta<sub>1-x</sub>Nb<sub>x</sub>O<sub>7</sub> system some oxygens are located in 24d (0.5, 0.25, 0.25) rather than the 48i site [19].

Our Rietveld refinements of Bi<sub>12.5</sub>Ln<sub>1.5</sub>ReO<sub>24.5</sub> (Ln = Lu, Er) indicate that the cations occupy the 4a (0 0 0) site and that anion positions can be modelled by partial occupancy of 8c and 32f sites (Table 1) while possible occupancy of the 48i position is less clear (Fig. 3).

Due to the complicated distribution of anions in these systems, we chose to represent it with nuclear densities obtained by the MEM/MPF methods instead of the classical split-atom system. The methods can provide precise nuclear/electron distribution, is less prone to termination ripples than Fourier methods, and can also give indications of conduction pathways [20].

After completion of the iterative MEM/MPF procedure, the reliability factors  $R_B$  (R-Bragg factor; also denoted by  $R_I$ ) and  $R_F$  (R-structure

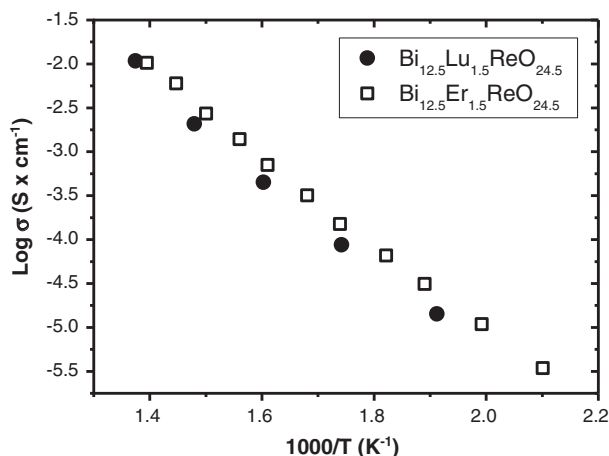


Fig. 1. Arrhenius plot of total conductivity for Bi<sub>12.5</sub>Lu<sub>1.5</sub>ReO<sub>24.5</sub> and Bi<sub>12.5</sub>Er<sub>1.5</sub>ReO<sub>24.5</sub>.

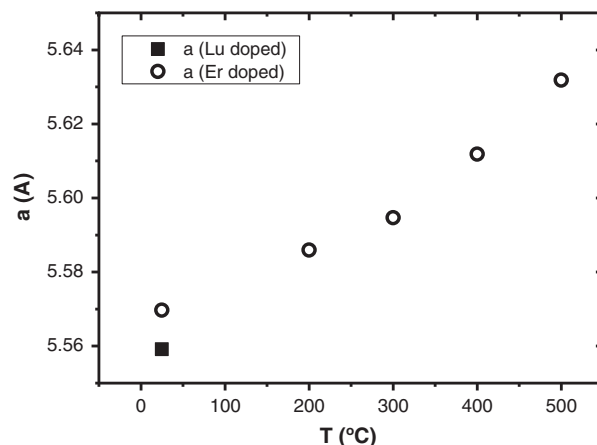


Fig. 2. Evolution of lattice parameter with temperature for Bi<sub>12.5</sub>Lu<sub>1.5</sub>ReO<sub>24.5</sub> and Bi<sub>12.5</sub>Er<sub>1.5</sub>ReO<sub>24.5</sub>.

factor) improved to final values of (%):  $R_B = 4.091$ ,  $R_F = 1.461$  (Bi<sub>12.5</sub>-Lu<sub>1.5</sub>ReO<sub>24.5</sub>, 25 °C);  $R_B = 2.844$ ,  $R_F = 1.024$  (Bi<sub>12.5</sub>Er<sub>1.5</sub>ReO<sub>24.5</sub>, 25 °C);  $R_B = 3.095$ ,  $R_F = 1.342$  (200 °C);  $R_B = 2.789$ ,  $R_F = 1.373$  (300 °C);  $R_B = 2.988$ ,  $R_F = 1.404$  (400 °C);  $R_B = 2.487$ ,  $R_F = 1.508$  (500 °C). MEM nuclear density distribution maps on the (110) plane of Bi<sub>12.5</sub>Lu<sub>1.5</sub>ReO<sub>24.5</sub> at 25 °C and Bi<sub>12.5</sub>Er<sub>1.5</sub>ReO<sub>24.5</sub> at various temperatures are displayed in Fig. 4. Examination of nuclear density distribution suggests some cation disorder with slight displacements from their ideal 4a position, but the most obvious feature concerns the disorder in oxide ions positions. As expected, the nuclear densities associated to oxide ions spread over a wide area, forming a continuous tetrahedral volume roughly covering the 8c and 32f positions, which is observed in other fluorite structured materials both experimentally [20,21] and theoretically [22]. This is observed at all studied temperatures and the extent of this volume increases with temperature, which is consistent with higher atomic displacement parameters at higher temperatures. Some differences can however be observed at different temperatures (Figs. 4 and 5).

At 200 – 300 °C: nuclear densities are localised in the tetrahedral volume roughly covering the 8c and 32f positions with “bulges” of nuclear densities pointing toward the 48i position, while at 400 and 500 °C continuous nuclear densities forming a straight line along the <100> direction are found, indicative of oxide-ion diffusion pathway along that direction. In the literature, curved pathways along the <100> direction passing through the 48i site are generally observed in fluorite materials [20], the prevalence of curve pathway as opposed from straight pathway is explained by the repulsion between cation and anions, the curved pathway allowing the cation–anion to maintain a reasonable distance. However, a straight pathway is observed for Y<sub>0.785</sub>Ta<sub>0.215</sub>O<sub>1.715</sub> [23], as is the case for the present material. This suggests that Ta and Re cations might play a similar role in these systems.

The direct oxide-ion diffusion pathway along the <100> direction is visible at 400 and 500 °C, with coherent scattering length of 0.21 f. Å<sup>-3</sup> at the 24d (0.5, 0.25, 0.25) site (distances cation – 24d site ~1.99 Å). Some density “bulges” from the tetrahedral volume covering the 8c and 32f sites pointing toward the <111> direction, and at the 24e (0.33 0 0) site, are also present. This suggests a possible supplementary curved conduction path along the <110> direction going through the 8c/32f – 24e – 8c/32f sites around the cation (distances cation – 24e site ~1.86 Å). Reducing the coherent scattering length to 0.11 f. Å<sup>-3</sup> allows visualising the pathway (Fig. 6).

It is interesting to note that the different nuclear densities associated to anion distribution at (i) 200–300 °C and (ii) 400–500 °C appear to reflect the non linear behaviour of atomic parameter variation with temperature. Non linear evolution of lattice parameter

**Table 1**

Final atomic positions for  $\text{Bi}_{12.5}\text{Lu}_{1.5}\text{ReO}_{24.5}$  (BiLu) and  $\text{Bi}_{12.5}\text{Er}_{1.5}\text{ReO}_{24.5}$  (BiEr) from Rietveld refinement. Space group  $Fm-3m$  (225); all cations in  $4a$  (0 0 0), O(1) in  $8c$  ( $\frac{1}{4} \frac{1}{4} \frac{1}{4}$ ), O(2) in  $32f$  ( $x x x$ ). Cations occupancies Bi/Ln/Re = 0.8333/0.1/0.0667.

	BiLu- 25 °C	BiEr- 25 °C	BiEr- 200 °C	BiEr- 300 °C	BiEr- 400 °C	BiEr- 500 °C
$a$ (Å)	5.5591(1)	5.5698(1)	5.5860(2)	5.5948(2)	5.6118(2)	5.6318(3)
$x$ $32f$	0.364(1)	0.368(1)	0.359(1)	0.356(1)	0.354(1)	0.354(1)
Occ O(1)	0.592(5)	0.586(5)	0.578(5)	0.568(5)	0.554(5)	0.554(6)
Occ O(2)	0.060(1)	0.053(1)	0.060(1)	0.062(1)	0.066(1)	0.066(1)
Uiso cations	4.55(4)	3.92(4)	5.33(3)	5.63(3)	6.21(4)	7.01(4)
Uiso oxygens	11.5(1)	10.2(1)	11.7(1)	11.8(1)	11.9(1)	12.6(1)
$\chi^2$ (47 var.)	2.409	2.780	3.478	3.304	2.887	2.696
Rwp	0.0246	0.0237	0.0274	0.0268	0.0251	0.0243

with temperature in  $\text{Bi}_3\text{Ta}_{0.50}\text{Nb}_{0.50}\text{O}_7$ , resulting in slightly higher than expected cell volume at higher temperature, has been explained by the increased occupancy at the  $24d$  position – which is interstitial to the cubic closed packed (ccp) fluorite lattice – at elevated temperatures [19]. Since in the present materials nuclear densities are observed at the  $24d$  site at 400 and 500 °C only, this explanation can also be applied to the present case.

#### 4. Conclusions

Both  $\text{Bi}_{12.5}\text{Lu}_{1.5}\text{ReO}_{24.5}$  and  $\text{Bi}_{12.5}\text{Er}_{1.5}\text{ReO}_{24.5}$  crystallise in the cubic  $\delta\text{-Bi}_2\text{O}_3$  type system. New information on the evolution with temperature in the oxygen sublattices of the highly disordered Bi–Ln–Re–O system has been collected. At 500 °C, an oxide ion diffusion pathway along  $\langle 100 \rangle$  is clearly observed. Contrarily to most  $\text{Bi}_2\text{O}_3$ –

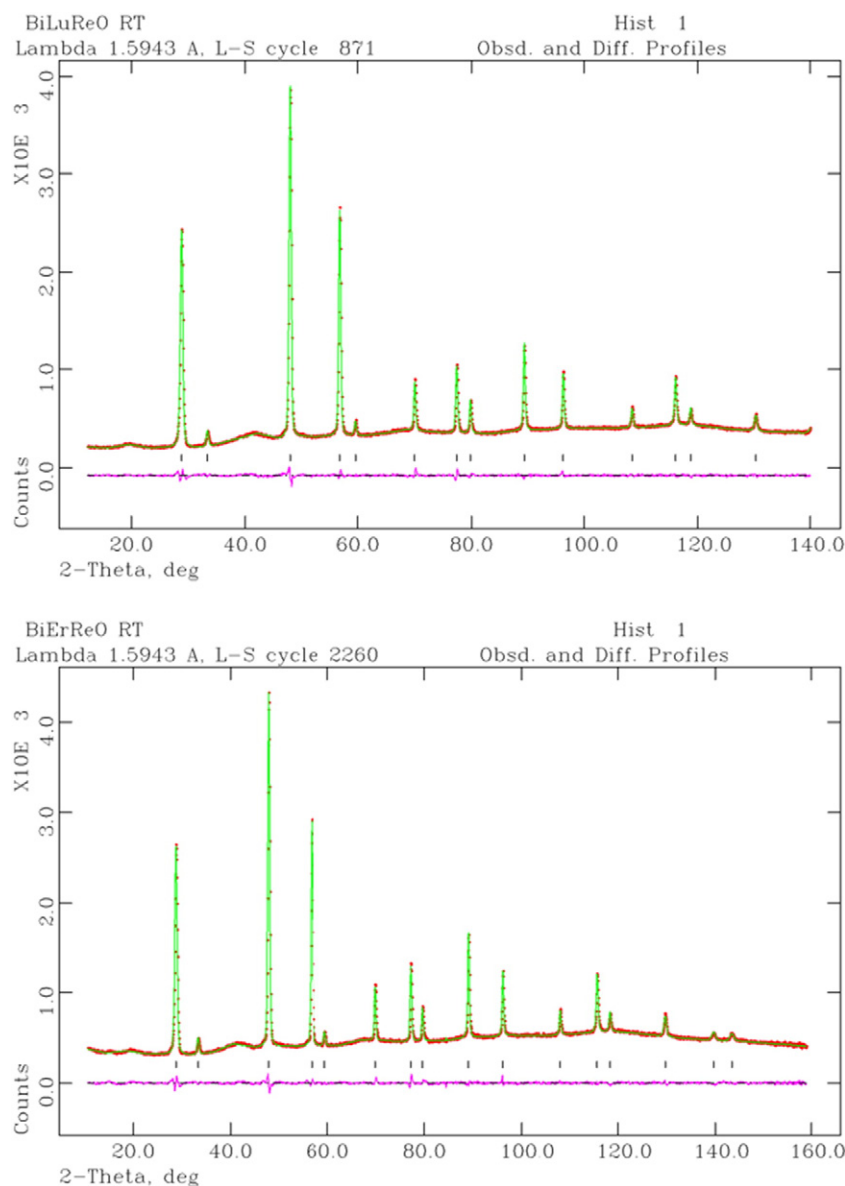


**Fig. 3.** Final Rietveld plot of a)  $\text{Bi}_{12.5}\text{Lu}_{1.5}\text{ReO}_{24.5}$  and b)  $\text{Bi}_{12.5}\text{Er}_{1.5}\text{ReO}_{24.5}$  at room temperature.



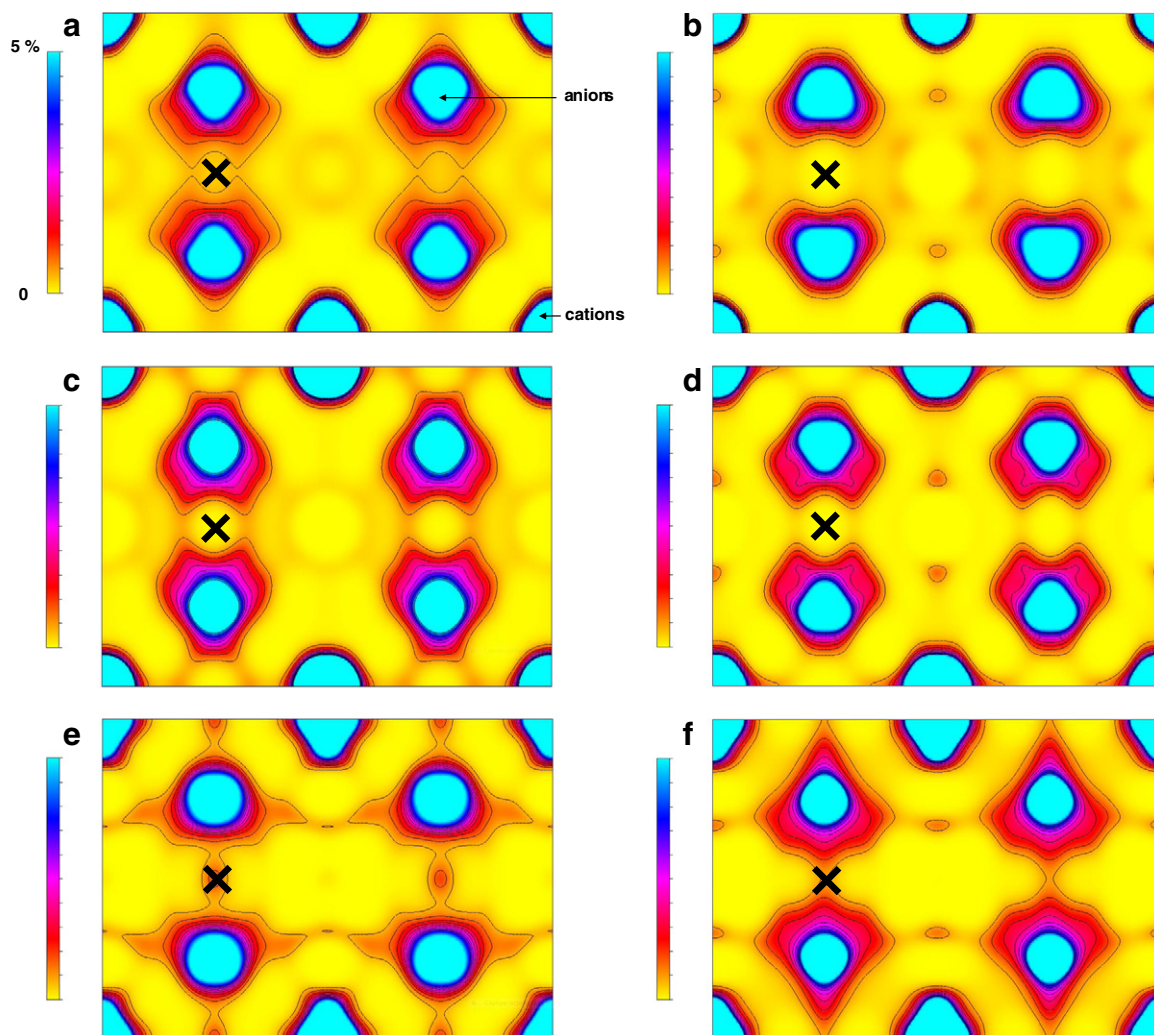


**Fig. 4.** Nuclear-density distribution on the (110) plane of a)  $\text{Bi}_{1.25}\text{Lu}_{1.5}\text{ReO}_{24.5}$  at 25 °C and  $\text{Bi}_{1.25}\text{Er}_{1.5}\text{ReO}_{24.5}$  at b) 25 °C, c) 200 °C, d) 300 °C, e) 400 °C, f) 500 °C. Saturation level 0 – 5%, with contours lines in the range 0.2 to 2 f. Å<sup>-3</sup> (0.2 f. Å<sup>-3</sup> step). The maximum densities corresponding to 100% are: for  $\text{Bi}_{1.25}\text{Lu}_{1.5}\text{ReO}_{24.5}$ : 53.91 f. Å<sup>-3</sup> at 25 °C, 38.31 f. Å<sup>-3</sup> at 200 °C, 44.52 f. Å<sup>-3</sup> at 300 °C, 53.20 f. Å<sup>-3</sup> at 400 °C, 43.32 f. Å<sup>-3</sup> at 500 °C. The black crosses indicate Wyckoff position 24d (0.5, 0.25, 0.25).

fluorite related systems, the pathway in the  $\langle 100 \rangle$  direction is not curved but straight. An additional pathway in the  $\langle 110 \rangle$  direction passing through the 24e ( $\sim 0.33\ 0\ 0$ ) site is also suggested. These features would explain the enhanced oxide ion conductivity observed in these materials.

### Acknowledgments

We thank EPSRC for financial support. We are grateful to Emmanuelle Suard at ILL for help with the collection of neutron diffraction data.

### References

- [1] G. Gattow, H. Schröder, Z. Anorg. Allg. Chem. 318 (1962) 176.
- [2] P.D. Battle, C.R.A. Catlow, J. Drennan, A.D. Murray, J. Phys. C 16 (1983) L561.
- [3] L.E. Depero, L. Sangaletti, J. Solid State Chem. 122 (1996) 439.
- [4] M. Yashima, D. Ishimura, Chem. Phys. Lett. 378 (2003) 395.
- [5] T. Takahashi, H. Iwahara, Mater. Res. Bull. 13 (1978) 1447.
- [6] J.C. Boivin, G. Mairesse, Chem. Mater. 10 (1998) 2870.
- [7] P. Shuk, H.-D. Wiemhöfer, U. Guth, W. Göpel, M. Greenblatt, Solid State Ionics 89 (1996) 179.
- [8] R. Punn, A.M. Feteira, D.C. Sinclair, C. Greaves, J. Am. Chem. Soc. 128 (2006) 15386.
- [9] R. Punn, I. Gameson, F. Berry, C. Greaves, J. Phys. Chem. Solids 69 (2008) 2687.
- [10] T.E. Crumpton, J.F.W. Mosselmans, C. Greaves, J. Mater. Chem. 15 (2005) 164.
- [11] C.H. Hervoches, C. Greaves, J. Mater. Chem. 20 (2010) 6759.
- [12] A.C. Larson, R.B. Von Dreele, General Structure Analysis System (GSAS), Los Alamos National Laboratory Report LAUR2004. 86–748.
- [13] B.H. Toby, J. Appl. Crystallogr. 34 (2001) 210–213.
- [14] F. Izumi, R.A. Dilanian, Recent Research Developments in Physics, Vol. 3, Part II, Transworld Research Network, Trivandrum, 2002, pp. 699–726.
- [15] F. Izumi, K. Momma, Solid State Phenom. 130 (2007) 15–20.
- [16] K. Momma, F. Izumi, J. Appl. Crystallogr. 44 (2011) 1272–1276.
- [17] S. Boyapati, E.D. Wachsman, B.C. Chakoumakos, Solid State Ionics 138 (2001) 293.
- [18] I. Abrahams, X. Liu, S. Hull, S.T. Norberg, F. Krok, A. Kozanecka-Szmigiel, M.S. Islam, S.J. Stokes, Chem. Mater. 22 (2010) 4435.
- [19] M. Struzik, X. Liu, I. Abrahams, F. Krok, M. Malys, J.R. Dygas, Solid State Ionics 218 (2012) 25–30.
- [20] M. Yashima, Solid State Ionics 179 (2008) 797–803.
- [21] S. Hull, S.T. Norberg, M.G. Tucker, S.G. Eriksson, C.E. Mohn, S. Stølen, Dalton Trans. (2009) 8737–8745.
- [22] C.E. Mohn, S. Stølen, S.T. Norberg, S. Hull, Phys. Rev. B 80 (2009) 024205.
- [23] M. Yashima, T. Tsuji, Chem. Mater. 19 (2007) 3539–3544.

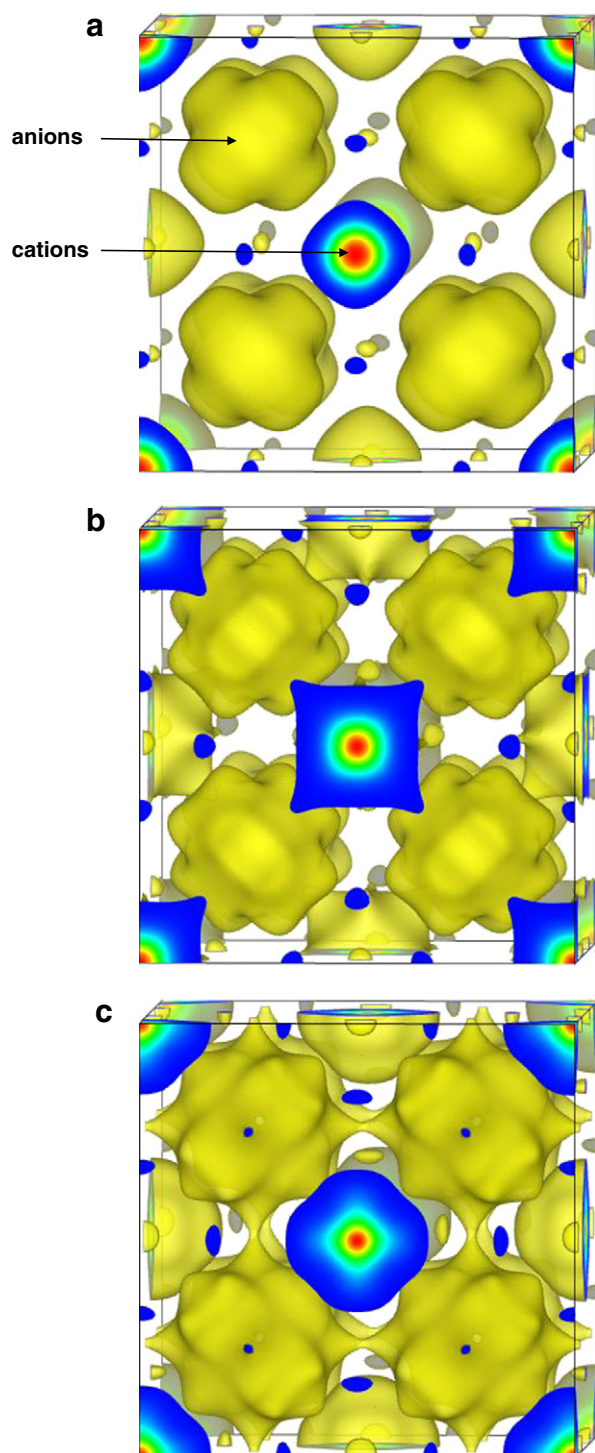


**Fig. 5.** 3D nuclear-density distribution of  $\text{Bi}_{12.5}\text{Er}_{1.5}\text{ReO}_{24.5}$  at a) 25 °C, b) 300 °C, c) 500 °C. ( $0.2 \text{ f. \AA}^{-3}$ ).

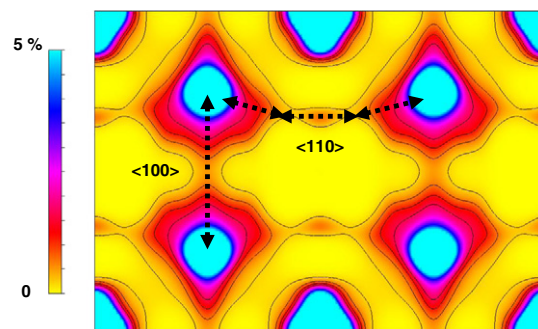


**Fig. 6.** Nuclear-density distribution on the (110) plane of  $\text{Bi}_{12.5}\text{Er}_{1.5}\text{ReO}_{24.5}$  at 500 °C. Saturation level 0 – 5%, with contours lines in the range  $0.1$  to  $2 \text{ f. \AA}^{-3}$  ( $0.2 \text{ f. \AA}^{-3}$  step). Arrows indicate apparent oxide ion diffusion paths along the 100 and 110 directions.